

Hydraulic performance and fouling characteristics of a membrane sequencing batch reactor (MSBR) for landfill leachate treatment under various operating conditions

Petros Gkotsis¹ · Jason Tsilogeorgis¹ · Anastasios Zouboulis¹ 

Received: 27 April 2017 / Accepted: 7 September 2017 / Published online: 13 September 2017
© Springer-Verlag GmbH Germany 2017

Abstract This study investigates the hydraulic performance and the fouling characteristics of a bench-scale membrane sequencing batch reactor (MSBR), treating mature landfill leachate under various time-based operating conditions. The MSBR system operated initially under a high-flux condition (Period 1) which resulted in a rapid trans-membrane pressure (TMP) rise due to intense fouling. Following the characterization of Period 1 as super-critical, the system was subsequently operated under a near-critical condition (Period 2). The overall filtration resistance analysis showed that cake layer formation was the dominant fouling mechanism during Period 1, contributing to 85.5% of the total resistance. However, regarding the MSBR operation during Period 2, adsorption was found to also be a dominant fouling mechanism (Days 1 to 47), contributing to 29.1% of the total resistance. Additionally, the irregular total resistance variation, which was observed during the subsequent operation (Days 48 to 75), and the respective filtration resistance analysis suggested also the formation of an initial sludge cake layer on the membrane surface, contributing to the 47.7% of the total resistance.

Keywords Membrane sequencing batch reactor (MSBR) · Landfill leachate treatment (mature) · Membrane fouling · Resistance-in-series model · Flux-step method

Nomenclature

COD	Chemical oxygen demand
EPS	Extracellular polymeric substances
HRT	Hydraulic retention time
MBR	Membrane bioreactor
MLSS	Mixed liquor suspended solids
MSBR	Membrane sequencing batch reactor
PAC	Powdered activated carbon
PVDF	Polyvinylidene fluoride
PWF	Pure water flux
SBR	Sequencing batch reactor
TMP	Trans-membrane pressure
TN	Total nitrogen

Introduction

Membrane sequencing batch reactors (MSBRs) offer an interesting alternative treatment option for wastewater treatment, as they combine the advantages of both SBR (sequencing batch reactor) and MBR (membrane bioreactor) technologies, namely readily changeable and easily controllable cycle operation, complete biomass rejection through membrane filtration (instead of the conventional sedimentation step), increased mixed liquor suspended solids (MLSS) concentration (therefore increased biological treatment kinetics and reduced aeration reactor volume), high-quality effluent, and smaller (than the conventional treatment systems) footprint. The ability to operate in a time, rather than in a space, sequence and the fact that operational variables can be easily adjusted to suit changing wastewater characteristics offer a high level of process flexibility in MSBR systems (Pajoumshariati et al. 2017; Xu et al. 2014; Laitinen et al. 2006). Another key feature of these systems is the complete decoupling of sludge age and hydraulic residence time which, in combination with the high MLSS

Responsible editor: Gerald Thouand

✉ Anastasios Zouboulis
zoubouli@chem.auth.gr

¹ School of Chemistry, Chemical and Environmental Technology Section, Aristotle University of Thessaloniki, Box 116, 54124 Thessaloniki, Greece

concentration, can result in almost an order of magnitude intensification of the biological process and lead to a substantial reduction of the reactor volume (Tsilogeorgis et al. 2008). In addition, the separation of biological sludge by means of a membrane leads to complete retention of biomass resulting in a high mixed liquor suspended solids concentration: this allows a very high treatment capacity especially for a submerged MSBR (Moreno-Andrade and Buitrón 2012).

On the other hand, membrane fouling remains the major bottleneck for all types of MBR systems (Wang et al. 2014; Huyskens et al. 2012). According to the IUPAC definition, fouling is a disturbing process, resulting in the loss of membrane performance, due to the deposition of suspended or dissolved substances on its external surfaces, as well as on or within the pore openings (IUPAC 1996).

It is well-understood that the extent of fouling in every membrane separation process depends on three fundamental factors: (1) the specific characteristics of the feed to be treated, (2) the membrane properties, and (3) the specific hydrodynamic conditions around the membrane (Qaisrani and Samhaber 2011; Fane 2006). In MBR systems, the interpretation of fouling characteristics, i.e., the identification and quantification of the various fouling components, can be far more challenging, than in most membrane applications, due to the complex interrelation of previous factors. Therefore, there is an ongoing need for the development of both theoretical and experimental effective research tools toward a better understanding of membrane fouling mechanisms.

To control membrane fouling and maintain a sustainable operation, the concept of critical flux in membrane bioreactors proposed by Field et al. (1995), who defined it as the specific flux value, below which the increase of trans-membrane pressure (TMP) with time (which is an important operational parameter of most membranes' operation), and under constant flux operation, does not occur anymore; noting that above this flux level, fouling can be immediately observed. Since then, the critical flux has been extensively applied to all membrane processes from microfiltration to reverse osmosis (Wang et al. 2008). The general trend is to reduce operational risk and to maintain sustainable permeability by operating at fluxes below the critical flux value, where fouling is (expected to be) limited (Vera et al. 2014; Li et al. 2013). Theoretically, when a membrane bioreactor operates below the critical flux, its permeate flux remains constant. In other words, fouling should not occur during the sub-critical flux operation. However, some researchers have shown that a dramatic increase in fouling rate can occur for some time, even when operating under sub-critical fluxes (Nguyen et al. 2014; Li et al. 2013).

Various methods have been encountered in the literature for the determination of critical flux (Nguyen et al. 2014; Wang et al. 2008), with the flux-step method being the most frequently used (Van der Marel et al. 2009). This method is based upon recording the TMP values, while the permeate flux is increased in a

stepwise manner during fixed time intervals. Therefore, it is possible to observe the transition from constant to non-constant permeability, i.e., from sub-critical to super-critical operation, simply by plotting flux and TMP values against time in the same graph. Recent studies suggest that this transition marks the boundary between fouling by the presence of extracellular polymeric substances (EPS) and by the sludge solids (Li et al. 2013). Fouling increases the membrane hydraulic resistance over time, resulting in the reduction of membrane permeability (Zhao et al. 2014). Total membrane filtration resistance, as defined by Darcy's law, is usually analyzed by using the resistance-in-series model to describe the specific contribution of each fouling mechanism (Zhang et al. 2015; Diez et al. 2014).

This study aims to investigate the hydraulic performance and the fouling characteristics of a bench-scale MSBR system, treating mature landfill leachate under various time-based treatment operating conditions. Leachate treated by conventional methods is hard to be allowed to discharge because it often contains hazardous organic contaminants, ammonia, heavy metals, and inorganic salts (Wang et al. 2014; Dong et al. 2014). The combination of biological degradation and physical separation achieved in the membrane bioreactor technology has shown satisfactory results in treating old/stabilized landfill leachates (Boonnorat et al. 2016; Hashisho et al. 2016; Niu et al. 2016). However, to the author's best knowledge, little information on the detailed correlation of different operating conditions with the corresponding dominant fouling mechanisms has been so far reported for these treatment systems. In this study, a MSBR operated under high-flux (Period 1) and near-critical flux (Period 2) conditions and the resistance-in-series fouling model was employed and thoroughly analyzed. In addition, the flux-step method was employed for the determination of the system's critical flux, to characterize the high-flux operating condition (during Period 1) as super-critical or not. The correlation of fouling mechanisms (cake layer formation, adsorption in membrane pores, etc.) with different operating conditions is expected to contribute to the effective design of prospective MBR treatment systems, especially when selecting the appropriate additives for fouling control; scouring agents, such as biofilm carriers or granular materials, can be used for the mitigation of reversible fouling (caused mainly by cake layer formation), while the use of adsorbent agents, such as powdered activated carbon (PAC), is preferable for the mitigation of irreversible fouling (caused mainly by inner pore blockage).

Materials and methods

MSBR operation and configuration

The bench-scale setup MSBR treatment unit (Fig. 1) consisted of a continuously stirred aerated bioreactor with a vertical-

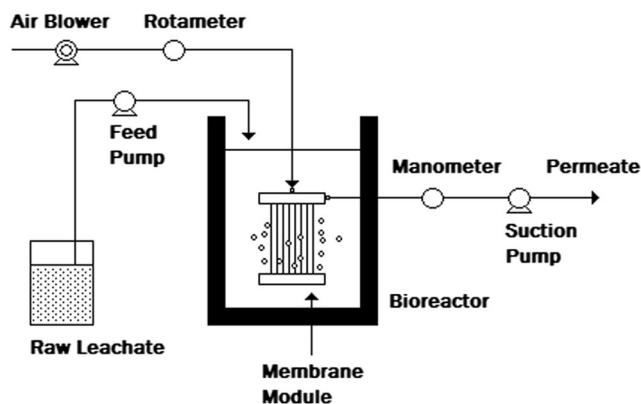


Fig. 1 Schematic layout of the MSBR experimental setup

mounted submerged membrane module. The bioreactor was a cylindrical Plexiglas-made vessel with a working volume of 5 L (diameter base 0.14 m, wet height 0.325 m). Raw (mature) leachate was fed to the MSBR by a small variable-rate peristaltic pump (Seko PR1). The permeate was withdrawn by a second peristaltic pump (Watson Marlow 503U), which was connected at the top header of the used membrane module. The TMP values were monitored on the screen of a pressure gauge (Kindmen), which was situated in the permeate line. Similarly to SBR systems, MSBRs are designed to operate under non-steady state flow conditions. Several operational cycles were examined during a 6-month experimental period. All these cycles consisted of four subsequent treatment steps, which were performed by means of programmable time switches in the following sequence: (1) fill, (2) react (applying alternative aerobic or anoxic periods), (3) membrane filtration, and (4) idle.

An ultrafiltration, hollow fiber membrane (ZW-1 model), manufactured by Zenon Environmental Inc., was used in this study (Table 1). The membrane module is equipped with a central aeration tube which was directly connected to the air transmission line. The tube supplied air close to the bottom header of the module, where orifices are located. Coarse bubbling was used both for scouring the accumulated colloidal

Table 1 Characteristics of the membrane used in the MSBR system (ZW-1 model)

Configuration	Hollow fiber, outside-in flow path
Material	PVDF
Nominal pore size	0.04 μm
Absolute rejection	0.1 μm
Nominal surface area	0.047 m^2
Maximum TMP limit	620 mbar
Typical TMP operating range	100–500 mbar
Typical pH operating range	5–9
Maximum OCl^- exposure	1000 mg L^{-1}

material off the membrane surface and for providing the biomass with the required oxygen concentration; the applied air flow rate was $0.34 \text{ m}^3 \text{ h}^{-1}$). Biomass (additional) mixing during the aerobic and anoxic operating periods was accomplished by a mechanical stirrer (not shown).

The bioreactor was initially inoculated with sufficient quantity of activated sludge, which was sampled from the recirculation channel of the municipal wastewater treatment plant of Thessaloniki (located near the town of Sindos). Prior to landfill leachate treatment tests, the MSBR unit was fed for over 3 months with synthetic wastewater of gradually increasing strength in terms of COD and TN concentrations, to examine the effect of influent (feed) characteristics on the system's operating performance. COD varied from 465 up to 4800 mg L^{-1} , whereas TN varied from 65 up to 570 mg L^{-1} . After the completion of the experiments with synthetic wastewater, the MSBR content was gradually replaced with (mature) landfill leachate feed. The replacement period lasted for 20 days, aiming for the acclimatization of biomass to the new influent characteristics.

Leachate feed and analytical methods

Several sampling campaigns were performed during the experimental period of 6 months. Leachate samples were received from the main municipal landfill site of Thessaloniki, which (at that time) was accepting $1000\text{--}1200 \text{ t day}^{-1}$ of municipal solid wastes. The produced leachate was collected in an artificial pond, which is located at the lowest part of the landfill. The main physico-chemical parameters of the landfill leachate which was used in the present study are shown in Table 2. Alkalinity and pH were determined according to the Standard Methods of APHA (1989), while chemical oxygen

Table 2 Main physico-chemical parameters of the mature landfill leachate used in these experiments

Parameter	Number of measurements	Min. value	Max. value	Mean value
pH	42	8.3	8.8	8.5
Alkalinity ($\text{mg CaCO}_3 \cdot \text{L}^{-1}$)	39	1474	2848	2028
Conductivity (mS cm^{-1})	20	10.8	11.5	11.3
Turbidity (NTU)	20	98	154	103
BOD (mg L^{-1})	6	155	250	197
COD (mg L^{-1})	39	1391	3977	2408
TN (mg L^{-1})	24	310	574	414
$\text{NH}_4^+ \text{-N}$ (mg L^{-1})	24	207	345	271
$\text{NO}_3^- \text{-N}$ (mg L^{-1})	23	7.7	25.4	15.1
$\text{PO}_4^{3-} \text{-P}$ (mg L^{-1})	26	5.2	13.7	7.8

demand (COD), total nitrogen (TN), ammonia (NH₄⁺-N), nitrate (NO₃⁻-N), and phosphate (PO₄³⁻-P) concentrations were measured with Hach Lange test kits. Unlike the pH and COD of young leachates which are generally found in the range of 4.5–6.5 and 30,000–60,000 mg/L, respectively (Umar et al. 2010), the relatively high pH values and the low COD concentrations clearly indicate a mature landfill leachate, which was partially stabilized in the open receiving pond.

Data processing and fouling assessment

The flux-step method was employed for the determination of the system’s critical flux value. Permeate flux was gradually increased for a set duration for each stage, resulting in relatively constant TMP values at lower fluxes and rising TMP values at fluxes higher than the critical flux. The desired permeate flux was achieved by measuring the volume of treated effluent per operational cycle. Temperature variations were considered by measuring the flux at a standard temperature (20 °C) according to the following equation (Yoon 2015):

$$JS = JM \left(\frac{\mu_M}{\mu_S} \right) \tag{1}$$

where, *J* is the permeate flux (L m⁻² h⁻¹, or LMH) and *μ* is the temperature-dependent permeate viscosity (mbar s). The subscripts M and S denote the measured and standard values, respectively (noting that the calculation of *μ_M* and *μ_S* values was based on pure water at the corresponding temperatures). The membrane filtration resistance was calculated, according to Darcy’s law, which describes the permeate flux through a porous membrane (Miller et al. 2014):

$$JS = \frac{\Delta P}{\mu_S R_t} \tag{2}$$

where, ΔP is the TMP (mbar) and R_t is the total filtration resistance (m⁻¹). Membrane fouling was described in detail by employing a four-parametric version of the resistance-in-series model:

$$JS = \frac{\Delta P}{\mu_S (R_m + R_f)} = \frac{\Delta P}{\mu_S (R_m + R_c + R_{ra} + R_{ia})} \tag{3}$$

where, the total resistance R_t is the sum of the intrinsic membrane resistance (R_m) and of the fouling resistance (R_f). The latter is considered to consist of three distinctive components, i.e., the cake layer resistance (R_c), the reversible adsorption resistance (R_{ra}), and the irreversible adsorption resistance (R_{ia}). R_c is caused by the accumulation of rejected solid particles near the membrane surface, whereas R_{ra} and R_{ia} are caused by the loose or strong attachment of soluble foulants to the membrane surface, respectively. Fouling characterization was achieved by carrying out filtration tests with pure water after each membrane cleaning step. R_c was assumed to be totally removed after rinsing the membrane with tap water. Similarly, R_{ra} was assumed to be totally removed after chemical cleaning of the membrane with the NaOCl solution. The methodology and the equations, which were applied for the calculation of all filtration resistance types, are presented in Table 3. Mixed liquor samples were analyzed for suspended solids concentration (MLSS) according to the Standard Methods of APHA (1989).

The membrane module was thoroughly cleaned between the various experimental periods. According to the implemented cleaning protocol, the external surface of the membrane was initially washed off with a sufficient quantity of tap water. Subsequently, the membrane module was soaked in 500 mg L⁻¹ of NaOCl solution at room temperature for 1 h with simultaneous air sparging. Using the NaOCl solution, membrane filtration was finally carried out for two different permeate flow rates, namely 0.36 L h⁻¹ for 50 min and 0.78 L h⁻¹ for 10 min (without aeration).

Table 3 Methodology and equations for the calculation of all resistance types

Resistance type	Determination method	Resistance type	Measured value	Equation
Total	Pure water filtration of fouled membrane	R_t	TMP, <i>J</i>	$R_t = \text{TMP}/(\mu J)$
Membrane	Pure water filtration of new (unused) membrane	R_m	–	$R_m = 9.59 \cdot 10^{11} \text{ m}^{-1}$
Fouling	–	R_f	–	$R_f = R_t - R_m$
Cake layer (R_c)	Pure water filtration of rinsed membrane	R_c	TMP', <i>J'</i>	$R' = R_m + R_{ra} + R_{ia} = \text{TMP}'/(\mu J')$, $R_c = R_t - R'$
Reversible adsorption	Pure water filtration of chemically cleaned membrane	R_{ra}	TMP'', <i>J''</i>	$R'' = R_m + R_{ia} = \text{TMP}''/(\mu J'')$, $R_{ra} = R' - R''$
Irreversible adsorption	–	R_{ia}	–	$R_{ia} = R_t - R_m - R_c - R_{ra}$

Table 4 Characteristics of the 24-h operational cycle during the MSBR operation at high flux (Period 1)

Days of operation	Total cycle time	Fill step time	React. step time	Filtration step time	Idle step time
0–4	24 h 0 min	1 h 20 min	20 h 30 min (NITRI only)	1 h 50 min	0 h 20 min
4–11	24 h 0 min	1 h 20 min	20 h 30 min = 18 h 30 min NITRI + 2 h 0 min DENI	1 h 50 min	0 h 20 min
11–18	24 h 0 min	1 h 20 min	20 h 30 min = 17 h 30 min NITRI + 3 h 0 min DENI	1 h 50 min	0 h 20 min

NITRI nitrification, DENI denitrification

Results and discussion

MSBR operation under high-flux condition

MSBR was initially operated under a high-flux condition for a period of 18 days (Period 1). The basic characteristics of operation during this period are shown in Table 4. Each cycle time totally lasted for 24 h (i.e., one treatment cycle/day). During the fill step, 500 mL of raw leachate was fed to the MSBR system. The filtration step consisted of suction and relaxation periods during which the suction to relaxation ratio was 1:1 (i.e., 10-min suction, 10-min relaxation). The HRT was 10 days and the air flow rate was $0.343 \text{ m}^3 \text{ h}^{-1}$. It must be stressed that sludge removal did not take place during that period, except for sampling reasons. Flux and permeate temperature variations during the high-flux operation period are presented in Fig. 2. The permeate temperature varied between 22 and 25 °C, whereas the flux varied between 8.9 and 9.5 LMH.

The total resistance (R_t) was correlated with the membrane's productivity, namely the permeate volume produced per unit of membrane area (Fig. 3). Initial R_t (iR_t) and final R_t (fR_t) values resulted from the corresponding TMP values, which were recorded 1 min after the beginning and the end of the filtration step, respectively. ΔR_t represents the amount of total resistance increase during the filtration step (i.e., $\Delta R_t = fR_t - iR_t$). Finally, the straight line represents the membrane resistance prior to immersion in the mixed liquor ($2.04 \cdot 10^{12} \text{ m}^{-1}$) and incorporates both R_m ($9.59 \cdot 10^{11} \text{ m}^{-1}$) and R_{ia} ($1.08 \cdot 10^{12} \text{ m}^{-1}$) values, where R_{ia} is caused by the

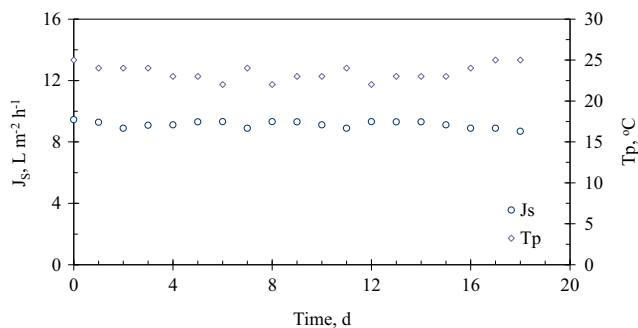


Fig. 2 Standard flux (J_s) and permeate temperature (T_p) variations during the MSBR operation under the applied high-flux operating condition

irreversible adsorption fouling due to the preliminary 3-month MSBR operation, when using synthetic wastewater.

As shown in Fig. 3, fR_t increased during the first filtration run ($8.74 \cdot 10^{12} \text{ m}^{-1}$). After the initial 11 days of relatively constant hydraulic operation with a mean value of $1.25 \cdot 10^{13} \text{ m}^{-1}$ (lag phase), fR_t started rising exponentially and finally reached the value of $1.78 \cdot 10^{13} \text{ m}^{-1}$ at the end of the last filtration run (exponential phase). This corresponds to a TMP value of 430 mbar, which is very close to the maximum TMP operation limit for the membrane (500 mbar). MSBR operation under these conditions is unfavorable, due to the substantial mechanical stress applied on the membrane hollow fibers, and the necessity for a more frequently applied cleaning protocol. The observed pattern of the total resistance can be explained by the rapid formation of a sludge cake layer around the membrane surface. This self-accelerating fouling process is caused by the application of a high-permeate flux operation. Therefore, once the initial fouling layer was formed, it continued to grow under the imposed high flux, regardless of a noticed slight decrease in the MLSS concentration of the aerated bioreactor, probably due to the sludge removal which took place for sampling reasons (Fig. 4). As shown in Fig. 4, the concentration of MLSS was not fully controlled; however, the removal of minor sludge amounts for sampling reasons contributed to the remaining MLSS concentration in a typical range encountered in most MBR applications ($7000\text{--}12,000 \text{ mg L}^{-1}$).

The dominant influence of cake layer formation on membrane fouling was showed by the calculation of all resistance types (Fig. 5). As shown in Fig. 5, R_c was as high as

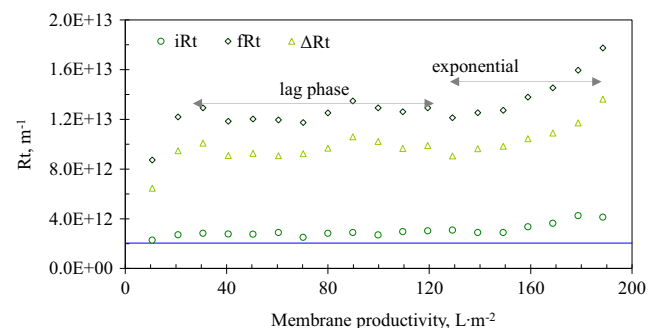


Fig. 3 Total resistance (R_t) with respect to membrane productivity during the MSBR operation under the high-flux operating condition

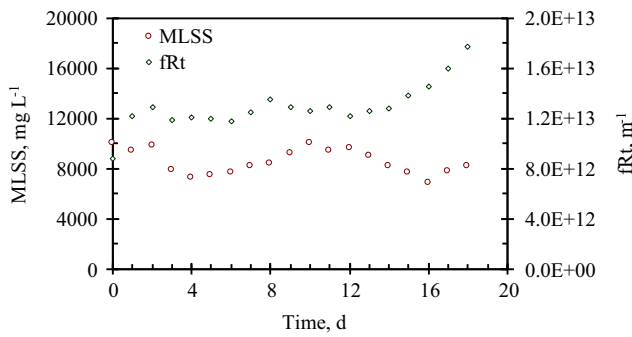


Fig. 4 Mixed liquor suspended solids (MLSSs) and final total resistance (fR_t) variations during the MSBR operation under the high-flux condition

$12.12 \cdot 10^{12} \text{ m}^{-1}$ and accounted for 91.7 and 85.5% of R_f and R_t , respectively. Fouling characterization also showed that R_{ra} was almost negligible (1.7% of R_t), whereas R_m and R_{ia} contributed almost the same to R_t (6.8 and 6.0% of R_t , respectively).

Critical flux determination

After the completion of Period 1, the critical flux was determined by the flux-step method (Fig. 6) aiming to explain the aforementioned results. A minimum flux-step of 2 LMH was used, determined by the suction pump specifications, while a 20-min step was selected. The MLSS concentration was 7000 mg L^{-1} , the permeate temperature was $25 \text{ }^\circ\text{C}$, and the air flow rate was $0.343 \text{ m}^3 \text{ h}^{-1}$.

As shown in Fig. 6, the TMP was constant ($dP/dt = 0$) for a flux up to 6.8 LMH (Steps 1–3), indicating zero fouling. However, even at very low imposed fluxes, fouling is still observed to some extent. The fact that no fouling was observed for the first 60 min of these experiments can be attributed to the low-pressure gauge sensitivity and to the short step duration. For the flux of 8.7 LMH (Step 4), the TMP shows a slight linear increase from 50 to 80 mbar ($dP/dt = 1.45 \text{ mbar min}^{-1}$). Finally, for the case of 10.7 LMH (Step 5), the TMP sharply increased from 90 to 240 mbar

Fig. 5 Resistance analysis after the MSBR operation under the high-flux condition

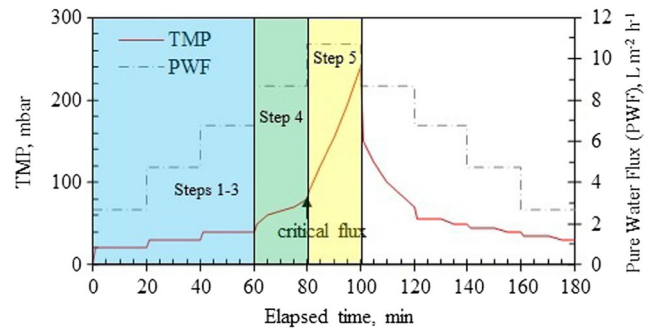
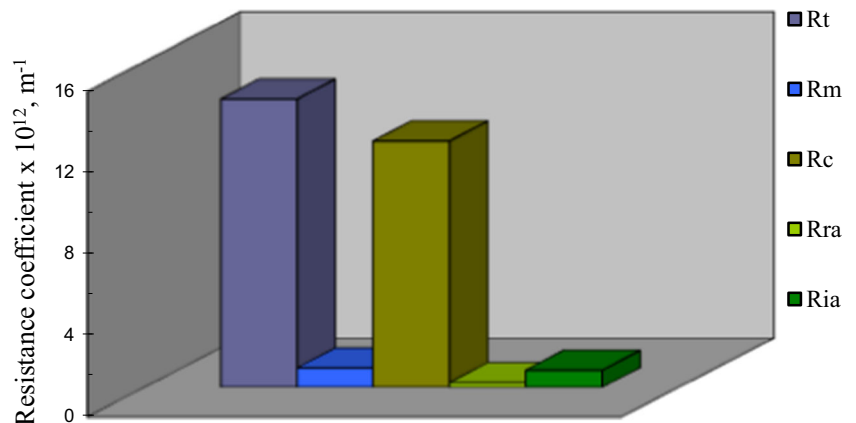


Fig. 6 Experimental determination of critical flux value by the application of flux-step method

($dP/dt = 7.82 \text{ mbar min}^{-1}$). Therefore, it can be assumed that the transition from the sub-critical to the super-critical operating condition took place near 8.7 LMH (or 7.7 LMH in terms of standard flux at $20.0 \text{ }^\circ\text{C}$). In fact, the critical flux is expected to be even lower than the recorded value of 8.7 LMH because the applied flux-step method was based on pure water flux (PWF, Fig. 6) instead of real permeate fluxes, i.e., after the filtration of mixed liquor.

The flux-step experiment was subsequently reversed to assess the fouling stability and reversibility. As shown in Fig. 6, the TMP values obtained during the descending phase were higher than the corresponding values which were recorded during the ascending phase. For example, during the fourth flux step of 8.7 LMH, the TMP increase rate was 1.45 and $4.14 \text{ mbar min}^{-1}$ for the ascending and descending phases, respectively. This hysteresis phenomenon reveals the influence of fouling history, indicating clearly that the membrane is not fully recovered from fouling during the descending phase (Navaratna and Jegatheesan 2011; Van der Marel et al. 2009). Similar observations were also reported by Le Clech et al. (2003), who developed the common flux-step method for fouling assessment in membrane bioreactors, operating under constant flux. The calculated critical flux of 8.7 LMH corresponds to MLSS concentration 7000 mg L^{-1} . Despite its dependence on the MLSS concentration (Dong et al. 2013; Wu et al. 2008), critical flux is a reliable parameter for

characterizing the system’s hydraulic performance. In this sense, the MSBR operation during Period 1 can be safely characterized as super-critical.

MSBR operation under the near-critical flux condition

The operation of MSBR under the near-critical flux condition was performed for a period of 75 days (Period 2). The basic characteristics of the operational cycles which were applied during this period are shown in Table 5. The total treatment cycle time was 12 h (2 cycles/day) for most experiments of this period. During the fill step, 250 mL of raw (mature) leachate was fed to the MSBR. The filtration step consisted of alternative suction and relaxation periods, with the ratio 1:3 (i.e., 5-min suction, 15-min relaxation). For an effluent volume of 250 mL and net filtration time of 40 min, the corresponding flux was 8.0 LMH which is very close to the calculated critical flux. The HRT was 10 days and the air flow rate was 0.343 m³ h⁻¹. Again, no sludge removal took place during this period, except for sampling reasons. The main operating conditions for Periods I and II are summarized in Table 6.

Flux and permeate temperature variations during the near-critical flux operation of MSBR treatment system are presented in Fig. 7. As shown, the permeate temperature decreased gradually due to seasonal changes, with the temperature decrease reaching 10 °C. However, the observed temperature variations present no adverse effect on the respective *J_S* values which increased with time. Due to the constant *J_S* increase, the system’s hydraulic performance was gradually shifted from the sub-critical to the super-critical zone (Day 25); nonetheless, it remained close to the critical condition (straight line in Fig. 7) until the 47th day of Period 2. During the following 23 days of operation, *J_S* variations became significantly greater, but it finally returned to the near-critical flux values after the 70th day.

As long as the system was operated closely to the critical hydraulic conditions, the *fR_t* was linearly increased with respect to membrane productivity (0–470 L m⁻²) (Fig. 8). A small *fR_t* “jump” from 5.15·10¹² to 6.41·10¹² m⁻¹ was observed at 480 L m⁻². However, for even higher productivity values, namely for hydraulic performance well beyond the critical condition, the pattern of linear resistance increase disappeared (possibly due to the rapid solids accumulation) and was replaced by irregular *fR_t* variations around the mean value of 6.72·10¹² m⁻¹.

As shown in Fig. 9, during the first 48 days of Period 2, the MLSS concentration varied between 6600 and 9400 mg L⁻¹, having a mean value of 7800 mg L⁻¹. However, during the remaining 27 days of MSBR operation, it was further increased from 9200 to 13,400 mg L⁻¹, noting that sludge was not actually removed during that period (except for sampling reasons).

Table 5 Characteristics of the 12-h treatment cycles during the MSBR operation under the near-critical flux condition (Period 2)

Days of operation	Total treatment time	Fill step time	React step time	Filtration step time	Idle step time
0–5	12 h 0 min	1 h 15 min	8 h 0 min = 7 h 0 min NITRI + 1 h 0 min DENI	2 h 25 min	0 h 20 min
5–8 and 11–15	12 h 0 min	1 h 15 min	8 h 0 min = 6 h 0 min NITRI + 2 h 0 min DENI, 9 h 0 min = 2 h 0 min NITRI + 1 h 0 min DENI + 2 h 0 min NITRI + 1 h 0 min DENI + 3 h 0 min NITRI	2 h 25 min	0 h 20 min
15–20	12 h 0 min	0 h 25 min	8 h 0 min (NITRI only)	2 h 25 min	0 h 20 min
20–25 and 28–29	12 h 0 min	1 h 15 min	8 h 0 min = 7 h 0 min NITRI + 1 h 0 min DENI	2 h 25 min	0 h 20 min
29–44, 46–52 and 53–55	12 h 0 min	1 h 15 min	8 h 0 min = 1 h 0 min DENI + 6 h 0 min NITRI + 1 h 0 min DENI	2 h 25 min	0 h 20 min
55–61	12 h 0 min	1 h 15 min	8 h 0 min = 3 h 0 min NITRI + 1 h 0 min DENI + 3 h 0 min DENI + 1 h 0 min DENI	2 h 25 min	0 h 20 min
61–75	12 h 0 min	1 h 15 min	8 h 0 min = 3 h 0 min NITRI + 1 h 0 min DENI + 3 h 0 min DENI + 1 h 0 min DENI	2 h 25 min	0 h 20 min

Table 6 Main operating conditions for Period I and Period II

	Period I	Period II
HRT, day	10	10
Air flow rate, m ³ h ⁻¹	0.343	0.343
Flux, LMH	8.9–9.5	7.8–8.2
Suction to relaxation ratio	1:1	1:3

The linear fR_t increase can be attributed to the adsorption of extracellular polymeric substances (EPS) on the membrane surface. Similar fouling behavior is common in continuous-flow, submerged MBR systems, which operate at well-defined sub-critical or near-critical hydraulic conditions. In such systems, the TMP increases with operation time almost linearly or occasionally slightly exponentially (Yoon 2015). The TMP increase rate (dP/dt) depends on both the imposed permeate flux and the production/deposition of EPS, which are widely considered to contribute to adsorption fouling, even under sub-critical operating conditions. For permeate fluxes which are well below the critical flux, the dP/dt can be very low resulting in a prolonged low-fouling MBR operation.

The irregular fR_t variation during the last 27 days of the near-critical MSBR operation indicates the presence of another dominant fouling mechanism, other than the adsorption. During this period, similarly to the super-critical MSBR operation (Figs. 2, 3, and 4), the combined effect of the super-critical J_S and the high MLSS concentration enabled the instant formation of an initial sludge cake layer on the membrane surface. Nonetheless, during the near-critical operation, the cake layer growth rate was lower than the corresponding one during the super-critical operation (Period 1). As already mentioned, during the super-critical operation (Period 1), the fR_t increased exponentially shortly after the onset of cake formation (Fig. 3). However, there was no similar increase during the cake-dominated phase of the near-critical flux condition (Period 2). This can be attributed to the different relaxation conditions experienced by the membrane hollow fibers during the super-critical or near-critical operation periods. The

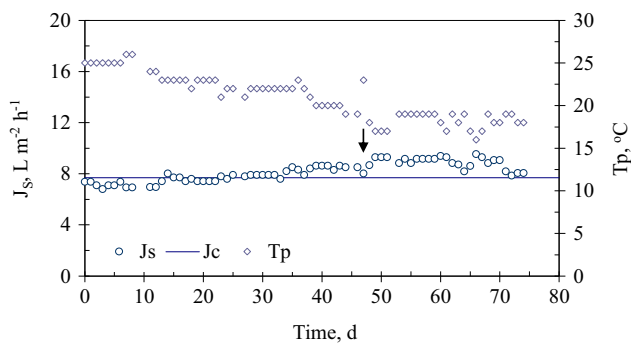


Fig. 7 Standard flux (J_S) and permeate temperature (T_p) variations during the MSBR operation under the near-critical flux condition (Period 2)

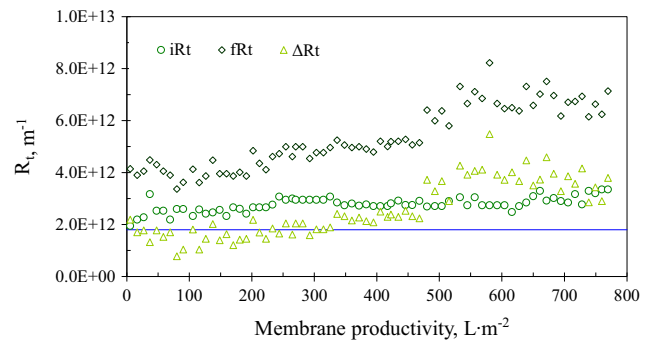


Fig. 8 Total resistance (R_t) with respect to membrane productivity during the MSBR operation under the near-critical MSBR operation (Period 2)

low suction to relaxation ratio which was applied in the near-critical flux condition allowed the greater removal of accumulated suspended solids from the membrane surface, and therefore, the slower development of the cake layer.

According to the resistance analysis (Fig. 10), the sum of R_{ra} and R_{ia} was equal to $1.20 \cdot 10^{12} \text{ m}^{-1}$ and accounted for 29.1% of R_t . Most of the adsorption resistance was developed mainly during the first 48 days of the near-critical operation where adsorption was the dominant fouling mechanism. On the other hand, R_c was as high as $1.97 \cdot 10^{12} \text{ m}^{-1}$ (47.7% of R_t). This was developed during the last 27 days of the near-critical MSBR operation, where cake formation became the prevailing fouling mechanism. Finally, R_m was responsible for 23.2% of R_t .

Lower MLSS concentration can be achieved by reducing the SRT (removal of larger amounts of sludge) resulting in the reduction of the cake layer as well. Attention must be paid, though, in order to avoid significant loss of solids, which may lead to MLSS concentration below the concentration limits of a typical MBR or MSBR system ($7\text{--}12 \text{ g L}^{-1}$). The application of back-pulse (back-washing) techniques can also be effective, regarding fouling mitigation, but their use is restricted mainly to hollow fiber membranes. The operation of such systems below the membrane’s critical flux together with the optimization of physical aeration protocols can be a reliable

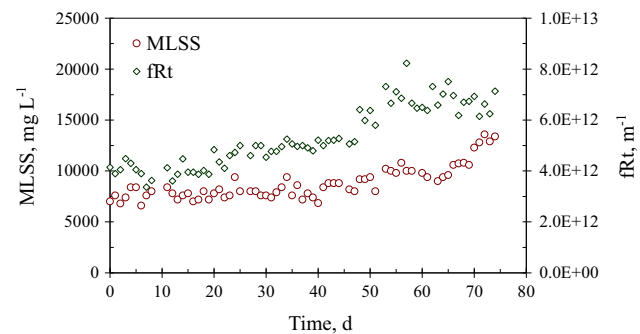


Fig. 9 Mixed liquor suspended solids (MLSS) and final total resistance (fR_t) variations during MSBR operation under the near-critical flux condition (Period 2)

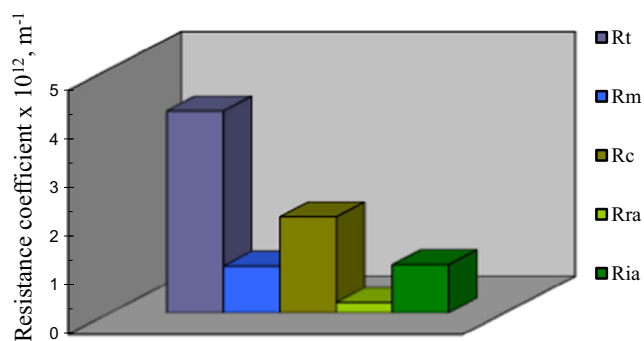


Fig. 10 Resistance analysis after the MSBR operation under the near-critical flux condition (Period 2)

method for reducing cake layer formation and membrane fouling in general.

Apart from the operation under low imposed fluxes and the application of high air rates for the effective scouring of the membrane's surface, the use of sludge additives is nowadays considered to be among the novel anti-fouling strategies with great potential and is strongly recommended. Due to their ability to alter and enhance sludge properties, the addition of several adsorbent or coagulant agents, such as powdered activated carbon or aluminum/ferric salts, has shown some promising results regarding fouling mitigation over the last few years. Future trends are also very likely to focus on their effect on different forms of fouling (i.e., reversible and irreversible fouling) in MSBR systems which is yet to be thoroughly examined.

Conclusions

Cake layer formation was the dominant fouling mechanism under the high-flux condition (Period 1), since it accounted for 85.5% of the total resistance. According to the obtained critical flux (8.7 LMH), the MSBR operation during Period 1 can be safely characterized as super-critical. The operation of MSBR system under the near-critical flux condition (Period 2) can be divided into two phases. As long as the system was operated closely to the critical condition (Days 1 to 47), the total resistance almost linearly increased with respect to membrane productivity. During this phase, the resistance analysis showed that adsorption was the dominant fouling mechanism, accounting for 29.1% of the total resistance. However, for hydraulic performance well beyond the critical condition (Days 48 to 75), the irregular total resistance variation, which was observed, indicated the presence of another dominant fouling mechanism, other than the previously mentioned adsorption. In this case, the combined effect of super-critical flux and of the high MLSS concentration enabled the instant formation of an initial sludge cake layer on the membrane surface, accounting for 47.7% of the total resistance.

References

- APHA (1989) Standard methods for the examination of water and wastewater. USA
- Boonnorat J, Chiemchaisri C, Chiemchaisri W, Yamamoto K (2016) Kinetics of phenolic and phthalic acid esters biodegradation in membrane bioreactor (MBR) treating municipal landfill leachate. *Chemosphere* 150:639–649
- Diez V, Ezquerro D, Cabezas JL, García A, Ramos C (2014) A modified method for evaluation of critical flux, fouling rate and in situ determination of resistance and compressibility in MBR under different fouling conditions. *J Membr Sci* 453:1–11
- Dong W, Wang X, Ye X, Wang Z, Zhang X (2013) Impact of operating conditions on the flux changing rate during dead-end microfiltration process. *Desal Wat Treat* 51:19–21
- Dong Y, Wang Z, Zhu C, Wang Q, Tang J, Wu Z (2014) A forward osmosis membrane system for the post-treatment of MBR-treated landfill leachate. *J Membr Sci* 471:192–200
- Fane AG (2006) Factors affecting fouling of MBR membranes. Proceedings of the MBR-Network Workshop on Bio-fouling in Membrane Systems, Norwegian University of Science and Technology (NTNU), Trondheim, Norway
- Field RW, Wu D, Howell JA, Gupta BB (1995) Critical flux concept for microfiltration fouling. *J Membr Sci* 100:259–272
- Hashisho J, El-Fadel M, Al-Hindi M, Salam D, Alameddine I (2016) Hollow fiber vs. flat sheet MBR for the treatment of high strength stabilized landfill leachate. *W Manag* 55:249–256
- Huyskens C, Wever HD, Fovet Y, Wegmann U, Diels L, Lenaerts S (2012) Screening of novel MBR fouling reducers: benchmarking with known fouling reducers and evaluation of their mechanism of action. *Sep Purif Technol* 95:49–57
- IUPAC (1996) Terminology for membranes and membrane processes. In: *Pure Appl Chem* 68:1479–1489
- Laitinen N, Loons A, Vilen J (2006) Landfill leachate treatment with sequencing batch reactor and membrane bioreactor. *Desalination* 191:86–91
- Le Clech P, Jefferson B, Chang IS, Judd S (2003) Critical flux determination by the flux-step method in a submerged membrane bioreactor. *J Membr Sci* 227:81–93
- Li J, Zhang X, Cheng F, Liu Y (2013) New insights into membrane fouling in submerged MBR under sub-critical flux condition. *Bioresour Technol* 137:404–408
- Miller DJ, Kasemset S, Paul DR, Freeman BD (2014) Comparison of membrane fouling at constant flux and constant transmembrane pressure conditions. *J Membr Sci* 454:505–515
- Moreno-Andrade I, Buitrón G (2012) Comparison of the performance of membrane and conventional sequencing batch reactors degrading 4-chlorophenol. *Water Air Soil Pollut* 223:2083–2091
- Navaratna D, Jegatheesan V (2011) Implications of short and long term critical flux experiments for laboratory-scale MBR operations. *Bioresour Technol* 102:5361–5369
- Nguyen TNP, Su YC, Pan JR, Huang C (2014) Comparison of membrane foulants occurred under different sub-critical flux conditions in a membrane bioreactor (MBR). *Bioresour Technol* 166:389–394
- Niu A, Ren YW, Yang L, Xie SL, Jia PP, Zhang JH, Wang X, Li J, Pei DS (2016) Toxicological characterization of a novel wastewater treatment process using EDTA-Na₂Zn as draw solution (DS) for the efficient treatment of MBR-treated landfill leachate. *Chemosphere* 155:100–108
- Pajoumshariati S, Zare N, Bonakdarpour B (2017) Considering membrane sequencing batch reactors for the biological treatment of petroleum refinery wastewaters. *J Membr Sci* 523:542–550
- Qaisrani TM, Samhaber WM (2011) Impact of gas bubbling and backflushing on fouling control and membrane cleaning. *Desalination* 266:154–161

- Tsilogeorgis J, Zouboulis A, Samaras P, Zamboulis D (2008) Application of a membrane sequencing batch reactor for landfill leachate treatment. *Desalination* 221:483–493
- Umar M, Abdul Aziz H, Suffian Yusoff M (2010) Variability of parameters involved in leachate pollution index and determination of LPI from four landfills in Malaysia. *Int J Chem Eng* 747953:1–6
- Van der Marel P, Zwijnenburg A, Kemperman A, Wessling M, Temmink H, Van der Meer W (2009) An improved flux-step method to determine the critical flux and the critical flux for irreversibility in a membrane bioreactor. *J Membr Sci* 332:24–29
- Vera L, González E, Díaz O, Delgado S (2014) Performance of a tertiary submerged membrane bioreactor operated at supra-critical fluxes. *J Membr Sci* 457:1–8
- Wang G, Fan Z, Wu D, Qin L, Zhang G, Gao C, Meng Q (2014) Anoxic/aerobic granular active carbon assisted MBR integrated with nanofiltration and reverse osmosis for advanced treatment of municipal landfill leachate. *Desalination* 349:136–144
- Wang Z, Wu Z, Yin X, Tian L (2008) Membrane fouling in a submerged membrane bioreactor (MBR) under sub-critical flux operation: membrane foulant and gel layer characterization. *J Membr Sci* 325:238–244
- Wu Z, Wang Z, Huang S, Mai S, Yang C, Wang X, Zhou Z (2008) Effects of various factors on critical flux in submerged membrane bioreactors for municipal wastewater treatment. *Sep Purif Technol* 62:56–63
- Xu S, Wu D, Hu Z (2014) Impact of hydraulic retention time on organic and nutrient removal in a membrane coupled sequencing batch reactor. *Water Res* 55:12–20
- Yoon SH (2015) *Membrane bioreactor processes: principles and applications*. CRC Press, USA
- Zhang Z, Wang Y, Leslie GL, Waite TD (2015) Effect of ferric and ferrous iron addition on phosphorus removal and fouling in submerged membrane bioreactors. *Water Res* 69:210–222
- Zhao C, Xu X, Chen J, Wang G, Yang F (2014) Highly effective anti-fouling performance of PVDF/graphene oxide composite membrane in membrane bioreactor (MBR) system. *Desalination* 340:59–66